

Human like motion generation for ergonomic assessment - a muscle driven Digital Human Model using muscle synergies

Marius Obentheuer^{1,2}, Michael Roller¹, Staffan Björkenstam³,
Karsten Berns², Joachim Linn¹

¹Fraunhofer Institute for Industrial
Mathematics, Fraunhofer Platz 1,
67633 Kaiserslautern, Germany
[Marius.Obentheuer, Michael.Roller,
Joachim.Linn]@itwm.fraunhofer.de

²Robotics Research Lab
Department of Computer Science
University of Kaiserslautern
Gottlieb-Daimler-Str.,
67663, Kaiserslautern, Germany
[obenth, berns]@rhrk.uni-kl.de

³Fraunhofer-Chalmers Centre
Chalmers Science Park,
SE-412 88, Gothenburg, Sweden
staffan.bjorkenstam@fcc.chalmers.se

Abstract

In this paper, an approach for digital human modelling and an appropriate simulation environment is presented. The human body or parts of it are modeled as a multibody system with Hill-type muscle models as actuators, and human like motions are created with an optimal control (OC) framework. The focus is on inner (muscle) loads for ergonomic assessment and human like motion generation. A basic reaching test is set up in a motion lab where muscle activation signals via EMG and upper body trajectories are measured with a motion capture system when performing a multitude of different reaching tasks. The measured data is used for validation of the simulation results and additionally muscle synergies are extracted from the EMG signals. These synergies can be used as control parameters in the musculoskeletal model, whereby the number of actuators is reduced. This leads to computational speedup, reduction of anatomical redundancy and captures human muscle activation profiles.

Keywords: Digital human model (DHM), musculoskeletal model, human motion, optimal control, DMOCC, muscle synergy, Hill muscle model

1. Introduction

Due to the ongoing demographic change, there is a growing need for individualization in high quality work places to prevent work related musculoskeletal disorders, especially in domains which still have a huge amount of manual work (e.g. assembly processes in automotive industry). Therefore, there is an increasing demand from industry for tools that can help develop safe and ergonomic workplaces. To be able to do ergonomic evaluations in early stages of a process (e.g. when developing tools or workstations), human motions and their interaction with the environment have to be included in the simulation process, which is a challenging task. It is a well-known problem when controlling complex multibody systems (MBS) that there is an infinite number of possible ways to move from a start configuration to an end configuration (kinematical redundancy). In biomechanical systems like musculoskeletal models the problem of anatomical redundancy has to be handled additionally. Here the number of actuators (muscles) in the model is higher than the number of kinematical degrees of freedom, which means that a specific motion can be generated by a multitude of different muscle actuations. Controlling a digital human model (DHM) in the scope of ergonomic assessment adds some constraints to the generated motions. On the one hand, the simulated task should be solved in a human like way, meaning that used forces, trajectories, velocities, accelerations etc. should be chosen in a way a real human might or at least could do it. Further on, it is important that the muscle activations for generating these motions are similar to those which the human central nervous system (CNS) would choose, as these data can be used to derive an assessment about how exhausting / ergonomic a motion (or repetitions of this motion, static postures...) will be for a human. Even though there are many possible options, humans use quite stereotypical muscle activations across individuals to create motions. A long standing question in neuroscience and other disciplines is how the CNS chooses these patterns and solves the redundancy problems. The CNS additionally has to handle the problem of neurological redundancy, meaning that a single muscle is innervated by several motor neurons [1].

One theory is that the CNS makes use of pre-defined building blocks (or modules) in the spinal cord which impose a specific pattern of muscle activation, known as motion primitives or muscle synergies. By linearly combining these modules, instead of explicitly activating every single muscle in particular, the dimensionality is reduced, which could simplify control while a wide range of motor outputs can still be produced [2]. Another (but not contradistinctive) approach to explain interindividual muscle activation patterns is the optimality principle which assumes that the CNS minimizes some kind of cost function, whereas the “costs” to be

minimized are not clear and there have been investigations on e.g. muscle activations, jerk, torque change, energy or time variance [3].

In our work we are not aiming on proving a control scheme of the CNS. Instead we concentrate on human like motion generation for ergonomic evaluation having a specific focus on inner loads and muscle activation signals. We use a DHM based on a full dynamic MBS model with *discrete mechanics and optimal control for constrained systems* (DMOCC) [4,5,6] which allows us to use, compare and combine the above described approaches in the application of human motion generation. The DHM can be actuated via joint torques, single muscles or muscle synergies. In Chapter 2, we give a short overview of our overall methods, the used MBS to model our DHM and the used OC code.

To get human motion data for validation and to study the spatial characteristics of human reaching movements we define and setup a *basic reaching test* in the motion lab. At this, the test subject stands in front of a plane and moves his hand (tip of middle finger) from a relaxed hanging start position to marked points on the plane. The test setup is adjusted to the test person's anthropometry. We measure 124 different motions including different distances and orientations to the plane, weighted motions and distinct final hand orientations. The surface electromyography (EMG) signals of 16 arm and shoulder muscles, as well as the arm/hand/shoulder trajectories are recorded with a motion capture system. In Chapter 3, the experimental setup and the data acquisition is described.

With a non-negative matrix factorization (NMF) algorithm [7], we extract *time invariant muscle synergies* (aka. *synchronous synergies*, *spatially fixed muscle synergies* or *muscle modes*) from the measured EMG data. The robustness of the extracted Synergies is evaluated by reconstructing the muscle activation signals of certain data sets using muscle synergies extracted from other data sets (different points and weights) and calculating the Variance Account For (VAF). The procedure for synergy extracting is described in Chapter 4. We then built up the basic reaching test in our DHM simulation environment and investigate the influence of different cost functions as well as the use of muscles and muscle synergies as actuators for the resulting motions (trajectories, velocities) and muscle activation signals. Our first simulation results are quite promising and give evidence that we follow an expedient approach that will lead to human like motions and provides natural muscle activation signals.

2. Concept / Approach

The majority of the state of the art DHM's for ergonomic assessment work with static postures and / or quasi-static motions. However, in many cases humans exploit kinetic quantities when fulfilling a task and consider (unconsciously) nonlinear properties of human force generation (e.g. force-length / force velocity dependency of muscles). This makes realistic human motions hard to predict with (quasi-) static models. Further on, those models do not deliver time and velocity information which are important quantities for ergonomic assessment methods. Additionally, even if the simulated trajectory (sequence of postures) is similar to a real dynamic trajectory, there can be a high diversity of inner loads, which might lead to wrong ergonomic estimations. In our approach, we work with a DHM based on a full dynamic MBS code with optimal control, which allows us to simulate dynamic tasks and to estimate the resulting forces and inner loads. Motions can be generated via three different actuation modes (AM1-AM3) which can be combined with each other (see Figure 1).

In AM1, the DHM is actuated via joint torques (t_i), meaning the OC code calculates a time series of t_i that minimize a certain cost function while fulfilling some motion constraints (e.g. start and end configuration of the DHM). The advantage of a joint torque driven model is that there is no anatomical redundancy problem, it calculates faster due to the reduced number of actuators compared to a muscle driven model, and it can be sufficient for motion evaluations like reachability, postures or time informations (e.g. to support and improve *methods-time measurement* (MTM) or similar methods). The main drawback of this actuation mode is that it does not deliver any information about inner forces.

In AM2, Hill-type muscles as in [5] are included in the MBS model and are used as actuators, such that the optimization produces a time series of muscle activation signals (a_i). This modelling delivers information about inner loads like e.g. muscle forces and the resulting loads to the human body, which can help to improve the ergonomic assessment of the simulated tasks. Additionally, using muscles as actuators can lead to more realistic and human like motions as it is oriented closer to the real human musculoskeletal system (hence, e.g. the OC system can exploit the nonlinear properties of human force generation).

In AM3, several muscles are grouped to muscles synergies (w_i), whereas the muscle activation signals result from the weighted and summed combination of all synergies. In this case, the optimization calculates the time series of the weights (c_i) for each synergy. The muscle synergies are extracted from measured EMG data as described in Chapter 4. Using muscle synergies as actuators reduces the problem of anatomical redundancy and can speed up calculation time. Additionally, muscle synergies capture the measured intermuscular coordination, such that using them as actuators could lead to more realistic muscle activation signals. For example, muscle co-

contraction is something that is hard to predict with classical optimization methods [8] but is indirectly included in the muscle synergies.

The actuation modes (AM1-AM3) can be combined with one another. So, e.g. muscles that could not be measured via EMG, and are therefore not included in any muscle synergy, can be activated solo. Or, if for some studies e.g. the inner loads of the upper extremity or the arm / hand are important, these parts could be modeled and actuated using AM2 or AM3, whereas the rest of the model can be actuated by AM1.

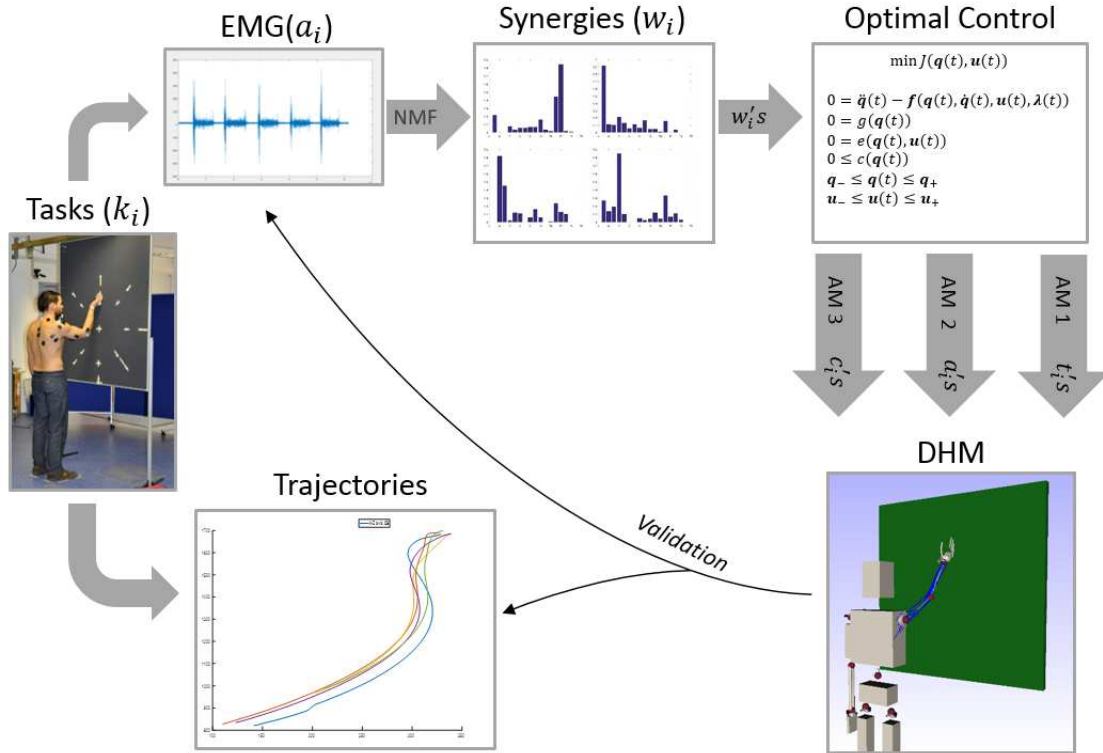


Figure 1: Overview of our DHM simulation environment and overall concept for human like motion generation; From tasks that are performed in the motion lab, EMG signals and trajectories are measured. From the EMG signals we extract muscle synergies that can be used as control parameters for the DHM. Depending on the actuation mode, the OC framework calculates a time series of muscle synergy weights, joint torques or muscle activations that fulfill the appropriate task. We can then compare the simulated trajectories and muscle activation signals with those measured in the motion lab when performing the same task and adjust the (mixed) OC cost function.

2.1. The DHM

In our work we use a (prototypical) MBS code based on [9] that uses minimal coordinates and facilitates fast computational algorithms to determine forces and velocities [10,11]. We are able to define rigid bodies (bones), joints and actuators freely adjusted to what we want to investigate. Depending on the created model, the resulting equation of motion for the MBS is an ordinary differential equation (for models with a tree-like structure) or a differential algebraic equation (for models containing closed loops). As actuators, we can specify motors (torques between rigid bodies) and hill-type muscles (force elements between rigid bodies). To estimate correct inner forces, the muscles are included in the simulation scenario. We use a string type Hill model as in [5] with a contractile component (CC) and a parallel elastic component (PEC) (see Figure 2). The CC creates a pulling force (F^m) depending on the actuation level, the length (l^m) and the contraction velocity of the muscle. The PEC, a (non-)linear spring which is connected in parallel to the CC, represents the passive stiffness of the tissue. The muscles are connected to the MBS through at least two body points (between which they build a straight line) and can be led over via points to adjust the muscle paths.

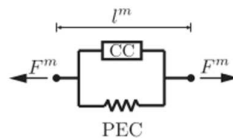


Figure 2: Rheological model of the simplified Hill-muscle

To simulate the basic reaching test, which is presented in this paper, we build up a 5 DOF model of the arm and shoulder as depicted in Figure 3. The shoulder is modeled as a spherical joint with three rotational DOFs. The shoulder anteversion, retroversion, adduction and abduction are nonlinearly constrained (the “bone” of the upper arm is restricted to lie in a defined cone) and the internal and the external rotation are limited with a box constraint (minimal and maximal angles). The elbow joint is modeled as two serial revolute joints where the flexion / extension as well as the supination / pronation of the forearm is limited with box constraints as well (minimal and maximal angles). As the test persons, which are performing the basic reaching test, are advised to keep the forearm, wrist and fingers stiff (see chapter 3), the bones of forearm and hand are modelled as one rigid body. As actuators, we define 5 motors (same axis as the rotational DOFs) and 29 muscles (blue and red lines in Figure 3)

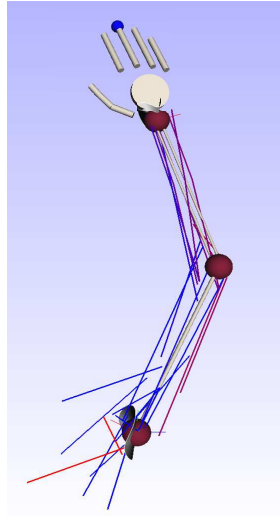


Figure 3: Test setup in our DHM simulation environment with a muscle driven model of the right arm. Upper arm, forearm and hand modeled as rigid bodies (grey) connected via joints (5 DOF, red balls with grey ellipsoids delimiting the range of motion) and actuated by hill-type muscle models (blue and red lines, 29 muscles).

2.2. The OC Code

The optimal control theory is a control strategy that is quite attractive in the application of DHM actuation. In principle, the OC code calculates the above described actuation signals (t_i , a_i , c_i) in a way, that a certain goal is fulfilled while minimizing some cost function(s) and considering the side constraints that the equations of motion of the MBS are fulfilled. In contrast to most other control strategies, the goal can be described in a quite generic manner and no further control signals have to be defined.

In our simulation environment, the time continuous OC problem is discretized by the DMOCC approach [6] where a variational integrator is used for the constraint equation of motion. The resulting finite dimensional optimization problem is solved with the interior point method implemented in the solver IPOPT [12]. As cost functions we implemented minimal time, minimal kinetic energy, minimal control and minimal control change. The cost functions can be linearly combined with one another to form a mixed cost function.

For the simulation of the *basic reaching test* (see chapter 3), the start posture (start configuration of the MBS) is set by determining the degrees of freedom of the MBS (corresponding to the start configuration of the test persons). As goal (end configuration of the MBS) we define the tip of the middle finger to be at a certain point in the room (target points of the basic reaching test, defined in the world coordinate system (WCS). Additionally the corresponding axis of the hand coordinate system (HCS) have to be in a certain angular range to the WCS to specify the final hand positions neutral, rotated inwards and rotated outwards. These angles are intentionally chosen to be in a wider range in order to let the OC code “choose” a “comfortable” solution as the test persons did while test execution.

All other motion parameters (trajectories, joint torques, muscle actuations etc.) result from the OC code. The described constraints were not changed when altering between the actuation modes (AM1-AM3).

3. The Basic Reaching Test

The basic reaching test is set up for two purposes. On the one hand, we want to identify the spatial characteristics of the muscle activation patterns generated by the CNS to control human reaching movements in a wide range of different motions. Therefore, we measure and analyze the EMG signals of 124 different reaching motions and extract *time invariant muscle synergies* as described in chapter 4. On the other hand, we use the measured motion data to validate our simulation results and to adjust the cost functions. We want to compare the resulting muscle

activation profiles of our musculoskeletal model with those measured at the basic reaching test to get realistic muscle activation profiles. Additionally, we want to compare the trajectories and velocity profiles which result from all simulation models (AM1 – AM3). Therefore, we measure the trajectories of thorax, shoulder, arm and hand with a motion capture system synchronized to the EMG signals.

Experiment design: The test person stands in front of a plane with 17 marked target points on it (Figure 4 *left*). The arrangement of these points is adjusted to the test persons anthropometry as depicted in Figure 4 *middle left*. The inner radius (R_i) corresponds to the upper arm length, the outer radius (R_a) equals 90% of the maximal reachability (R_{max_reach}) of the test person. The maximal reachability is estimated, in frontal position and in distance d_1 (see below) to the test plane, as follows: The subjected is instructed to move the tip of the middle finger to the highest reachable point on the plane while keeping his trunk and the center of the shoulder joint in position. This is repeated for the lowest reachable point as well as those being most far to the right and the left on the horizontal line in the height of the shoulder. From the four resulting distances the smallest one is defined as R_{max_reach} (whereas all of them are in the same range). The target points are placed on the intersections of R_i and R_a with the horizontal and the vertical lines and their bisectrices. The center of R_i and R_a is positioned concentric with the center of the shoulder joint (projected to the plane) in a relaxed and upright standing position. We specify two distances between the plane and the test person (d_1 and d_2) which are also determined based on the users anthropometry as shown in Figure 4 *middle right*. Distance d_1 corresponds to the length of the forearm whereas d_2 is defined as the distance between the subject and the plane when standing in a frontal position to the plane with the forearm parallel to the ground and the angle $\alpha = 45^\circ$ between the upper arm and the subjects coronal plane.

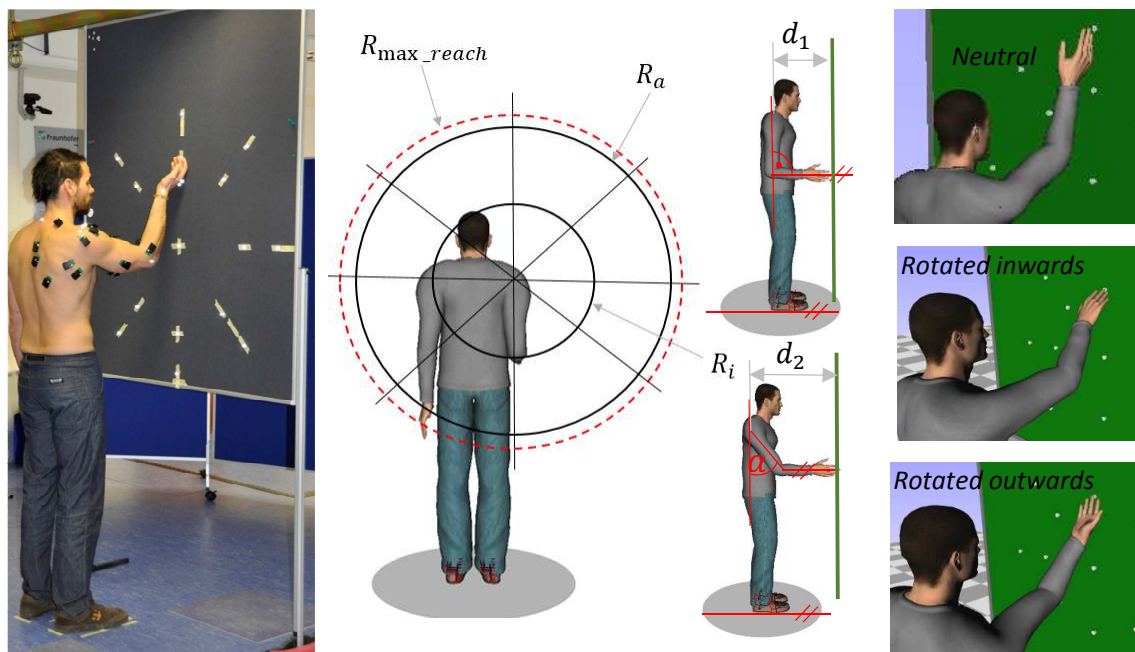


Figure 4: The Basic reaching test: (*left*) Test execution in the motion lab; (*middle left*) the three final hand orientations; (*middle right*) adaption of the target point placement to the test persons anthropometry; (*right*) distances d_1 and d_2 to the measuring plane, adapted to the test persons anthropometry

Test execution: We perform twelve different test scenarios, which are shown in Table 1. In all scenarios the test persons are instructed to stand in a straight and upright posture at the marked positions on the ground with the arms hanging relaxed in a natural position. We make tests from two distances (d_1 and d_2) and two distinct orientations to the test plane (frontal and lateral). In the frontal positions the subjects coronal plane is parallel to the test plane, in lateral positions the subjects sagittal plane is parallel to the test plane (right arm oriented towards the test plane). The test persons are instructed to move the tip of the middle finger (after the start signal) quickly to the target point on the plane and keep it in the final position for about one second. We define three final hand orientations: Neutral (N), rotated inwards (IRO) and rotated outwards (ORO) as seen in Figure 4. Additionally we make measurements with a weight cuff adjusted to the test persons wrist (1kg). Each task is repeated five times. The start signal just indicates that data recording started, the timing (start, end, holding time) for each repetition is not restricted by signals and freely chosen by the test persons. The subjects are advised to keep shoulder and trunk in position while moving the arm. A palmar flexion and a dorsal extension of hand and fingers as well as an ulnar abduction and a radial abduction should be avoided (which means that the forearm,

hand and fingers should be kept stiff as one rigid body). The motions are not restricted by any kind of apparatus to keep them natural.

Table 1: The different scenarios of the basic reaching test

	<i>Distance</i>	<i>weight</i>	<i>Orientation</i>	<i>Target Points</i>	<i>Hand positions</i>
<i>Test scenario 1</i>	d_1	No	Frontal	17 (P1-P17)	N
<i>Test scenario 2</i>	d_1	No	Frontal	17 (P1-P17)	IRO
<i>Test scenario 3</i>	d_1	No	Frontal	17 (P1-P17)	ORO
<i>Test scenario 4</i>	d_2	No	Frontal	9 (P9-P17)	N
<i>Test scenario 5</i>	d_2	No	Frontal	9 (P9-P17)	IRO
<i>Test scenario 6</i>	d_2	No	Frontal	9 (P9-P17)	ORO
<i>Test scenario 7</i>	d_2	No	Lateral	5 (P1,P5,P9,P13,P17)	N
<i>Test scenario 8</i>	d_2	No	Lateral	5 (P1,P5,P9,P13,P17)	IRO
<i>Test scenario 9</i>	d_2	No	Lateral	5 (P1,P5,P9,P13,P17)	ORO
<i>Test scenario 10</i>	d_1	Yes	Frontal	17 (P1-P17)	N
<i>Test scenario 11</i>	d_2	Yes	Frontal	9 (P9-P17)	N
<i>Test scenario 12</i>	d_2	Yes	Lateral	5 (P1,P5,P9,P13,P17)	N

In the test scenarios 1 to 3 the subjects are standing in frontal position to the test plane in distance d_1 . Target motions to all 17 target points are measured, each point with the three final hand orientations and without weight. The labeling of the target points is depicted in Figure 5. In the scenarios 4 to 6 the subjects are standing in frontal position to the test plane in distance d_2 . As the maximal reachability is determined in distance d_1 , only the target points on the inner circle (P9-P17) are measured. Again each point with the three above described different final hand orientations and without extra weight. In scenario 7 to 9 the subjects are standing in lateral position to the test plane in distance d_2 . Target motions to the target points on the vertical line are measured (P1, P5, P9, P13, P17), each point with the three different final hand positions and without weight. In scenarios 10 - 12 we made measurements with the weight cuff adjusted to the subjects hands. In scenario 10 the subjects are standing in frontal position to the test plane in distance d_1 and target motions to all 17 target points are measured with a neutral final hand position. In test scenario 11 the subjects were standing in frontal position to the test plane in distance d_2 and target points on the inner circle (P9-P17) are measured with a neutral final hand position. In the last scenario the subjects are standing in lateral position to the test plane in distance d_2 and target motions to the points on the vertical line are measured (P1, P5, P9, P13, P17) with a neutral final hand position. In sum, we measure 124 distinct motions (tasks) whereas every motion is repeated and recorded five times (repetitions).

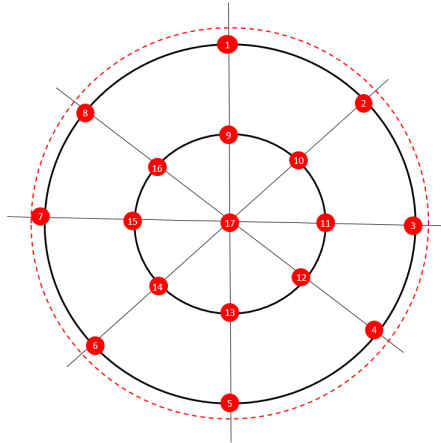


Figure 5: labeling of the target points

We additionally estimate the values for the maximal voluntary contraction (MVC) of the measured muscles. Therefore we measure the EMG values when performing the MVC tests as described in [13].

Data acquisition: In all test scenarios the position of the right hand, forearm, upper arm, shoulder and the thorax as well as the placement of the target points and the activity of 16 involved arm and shoulder muscles are recorded. The positions are tracked with an optical motion capture system (Qualisys, 9 cameras, Oqus 400 and Oqus 310+) with an accuracy of $< 1\text{mm}$ and a sample frequency of 240Hz. The Markers on the test persons are placed according to the recommendations of the international society of Biomechanics (ISB) as described in [14]. Palpation of anatomical landmarks is accomplished manually, following the guidelines of [15]. We additionally place a marker on each of the 17 target points on the test plane to be able to assess the characteristics

of close-to-goal velocities / trajectories and the influence of motion precision. The surface EMG signals are acquired with a wireless 16-channel Delsys system with a sample frequency of 2000Hz. The measured muscles are listed in Table 2. The EMG sensor locations were chosen following the recommendations of SENIAM and Konrad [13, 16, 17]. Before applying the sensors, the skin is shaved, cleaned with alcohol and rubbed with abrasive gel as recommended in [17]. Data recording (motion data as well as EMG signals) for each task started with a signal about one second before the first motion and was recorded continuously during all repetitions of each task.

Table 2: List of measured muscled

EMG Sensor	Muscle	Short name
01	M. trapezius desc.	TraDesc
02	M. trapezius transv.	TraTrans
03	M. trapezius ascend.	TraAsc
04	M. deltoideus clavicularis (ant.)	DeltAnt
05	M. deltoideus acromialis (med.)	DeltMed
06	M. deltoideus spinalis (post.)	DeltPost
07	M. biceps brachii	Bic
08	M. triceps brachii longus	TriLong
09	M. triceps brachii lateralis	TriLat
10	M. brachioradialis	BrRad
11	M. pectorialis major clavic.	PectClav
12	M. pectorialis major sternal	PectSter
13	M. infraspinatus	InfraSp
14	M. teres major	TeresM
15	M. latissimus dorsi	LatDors
16	M. pronator teres	PronTer

The basic reaching test is executed with two right handed males in the age of 25 and 35 after giving their informed consent. No (pre-existing) injuries or impairments of the skeletal and locomotor system of the arm and upper body were known at the time of test execution.

4. Muscle Synergies Extraction

The muscle synergy hypothesis is one approach to explain how the CNS might simplify motor control. There have been several investigations on humans and animals, which give evidence to suggest that the CNS makes use of a modular organization of the underlying motor circuits, which would reduce the number of degrees of freedom which have to be specified [2,7]. One representation for such a modular organization are *time invariant muscle synergies*, whereas one synergy stands for a group of muscles which can be activated synchronously in a fixed balance that does not change over time. By linearly combining the weighted outputs of each involved synergy, a specific motor output is generated. The muscle activations for a specific motor task would then be described by

$$\vec{a}(t) = \sum_{i=1}^n c_i(t) \vec{w}_i,$$

where \vec{a} is a vector that contains the activity values for each involved muscle, n is the number of synergies involved in this task, the weight c_i is a non-negative scalar value that indicates how active the synergy \vec{w}_i is, and \vec{w}_i is a vector containing the fixed balance of activity values for each muscles in this synergy. As the underlying synergies for human motion generation cannot be determined or identified in a direct way, a mediate method to estimate muscle synergies from the measured EMG signals evolved. Commonly some kind of factorization algorithm is used to identify a set of basis vectors, which can reproduce the measured EMG signals in an appropriate way.

In our work, we are not aiming on proving or falsifying the muscle synergy hypothesis for human motion generation. Instead, we want to use muscle synergies extracted from human motion data to actuate our DHM, which might bring several advantages. Of course, on the one hand, it is a promising way to build up a musculoskeletal model with an actuation method being as close to nature as possible if the focus is on muscle actuation profiles and inner loads. However, even if the human CNS does not make use of a (fixed) modular organization of the underlying motor circuits, the use of muscle synergies extracted from real motion data can still be quite attractive as actuation principle for a DHM. From a mathematical point of view, it is obvious that time invariant muscle synergies have two valuable properties. For one, they capture the spatial regularities of the measured EMG data, which is important information, and could help to produce more realistic muscle actuation

profiles (e.g. is a muscle co-contraction in parts already contained in the synergies, which is hard to predict using optimization methods and single muscles as actuators). Further on, the use of muscle synergies reduces the number of actuators which simplifies control and reduces the calculation time. Having in mind that the number of actuators is rising drastically when using muscles instead of joint torques as actuators, this can be exploited for speeding up calculation time as well as for reducing the problem of anatomical redundancy.

Data processing: The raw EMG signals are processed in a customized software written in *Matlab* (Mathworks). As described in the previous chapter, the EMG data is acquired continuously during execution of all five repetitions of each tasks. The signals are then separated repetition-wise into single sequences by visually identifying the start and the end of each motion. As start, we define the first visible movement of the arm / shoulder from the hanging rest position, and the end of the motion is defined as the moment when the tip of the middle finger reaches the target point and movement comes to rest. In order to capture all EMG signals potentially involved in the motion generation process, 200 frames ($\pm 0,1s$) before the first visible movement and after reaching the final hand position are included in each sequence. The EMG signals of each sequence are zero calibrated (by subtracting out the mean values), full wave rectified and low pass filtered (butterworth filter, cut off frequency 5 Hz, filter order 2). The EMG signals of each repetition are then arranged in a Matrix R_i (size t_R by n_m , where n_m is the number of measured muscles and t_R is the number of time samples of this repetition), that are concatenated vertically to the Matrix M_a which contains all measured tasks. We then apply a NMF algorithm to the Matrix M_a providing two matrices C_i and W_i such that

$$M_a = \begin{bmatrix} R_1 \\ \vdots \\ R_n \end{bmatrix}; M_a = \sum_1^{n_s} C_i * W_i + residuals,$$

where C_i is a Matrix (size t_a by n_s , where t_a is the number of time samples for all tasks and n_s is the number of synergies) containing the weights to approximate the measured EMG signals (M_a) by multiplying them with the synergy Matrix W_i (size n_s by n_m). The number of synergies (n_s) is a free parameter of the NMF algorithm and has to be chosen beforehand. This is generally done by calculating the variance account for (VAF) for a multitude of numbers of synergies and selecting a value for n_s where a certain threshold is reached (commonly 90% VAF) or the graph of the cumulative VAF presents a significant change of slope.

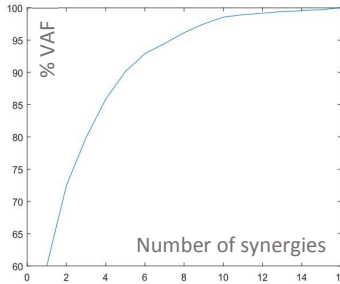


Figure 6: Variance Account For

We calculate the VAF (see Figure 6) as described in [18] for values of n_s between one and sixteen (each by running nmf 25 times to prevent it to converge to a local minima). The 90% VAF threshold is reached already with five synergies, which would reduce the number of actuators by two thirds. In our simulations, we work with different values for n_s and investigate the influence on the resulting (simulated) muscle activation signals. Additionally we validate the chosen values for n_s on the input-space side (measured muscle activation signals). Therefore, we extract muscle synergies from the Matrix M_c , which contains only muscle signals from reaching motions to those points which are placed on the horizontal and the vertical line (P1, P3, P13, P05, P07, P09, P11, P13, P15, P17) and used these synergies to reproduce the muscle signals measured from target points placed on the diagonal lines (P2, P4, P6, P8, P10, P13, P14, P16). To calculate appropriate weights (Matrix C_i) to approximate these muscle signals (M_c), we use a least-square fit algorithm with non-negative values. The same procedure we apply to the Matrix M_{nw} , which contains only measurements of motions without weight-cuff. We then use the here extracted synergies to reproduce the muscle signals measured when doing motions with weight cuff adjusted to the test persons wrist. In Figure 7 the results for $n_s = 10$ are show. The measured EMG signals, normalized to the MVC values of the respective muscle (vertical axis), are plotted with respect to time (horizontal axis: frames with framerate = 100Hz).

As one can see, the measured signals have a clear characteristic that is preserved over several repetitions, which indicates that the muscle activation signals are not just artefacts of measurement methods or noise. Further on, the muscle activation signals can be very well reproduced by using the extracted muscle synergies, even in those cases where the reproduced signals are not included in the NMF algorithm. Shown are the measured and reproduced EMG signals of the *musculus biceps brachi* (first column), *musculus triceps brachii lateralis* (second column) and *musculus deltoideus clavicularis* (anterior) (third column).

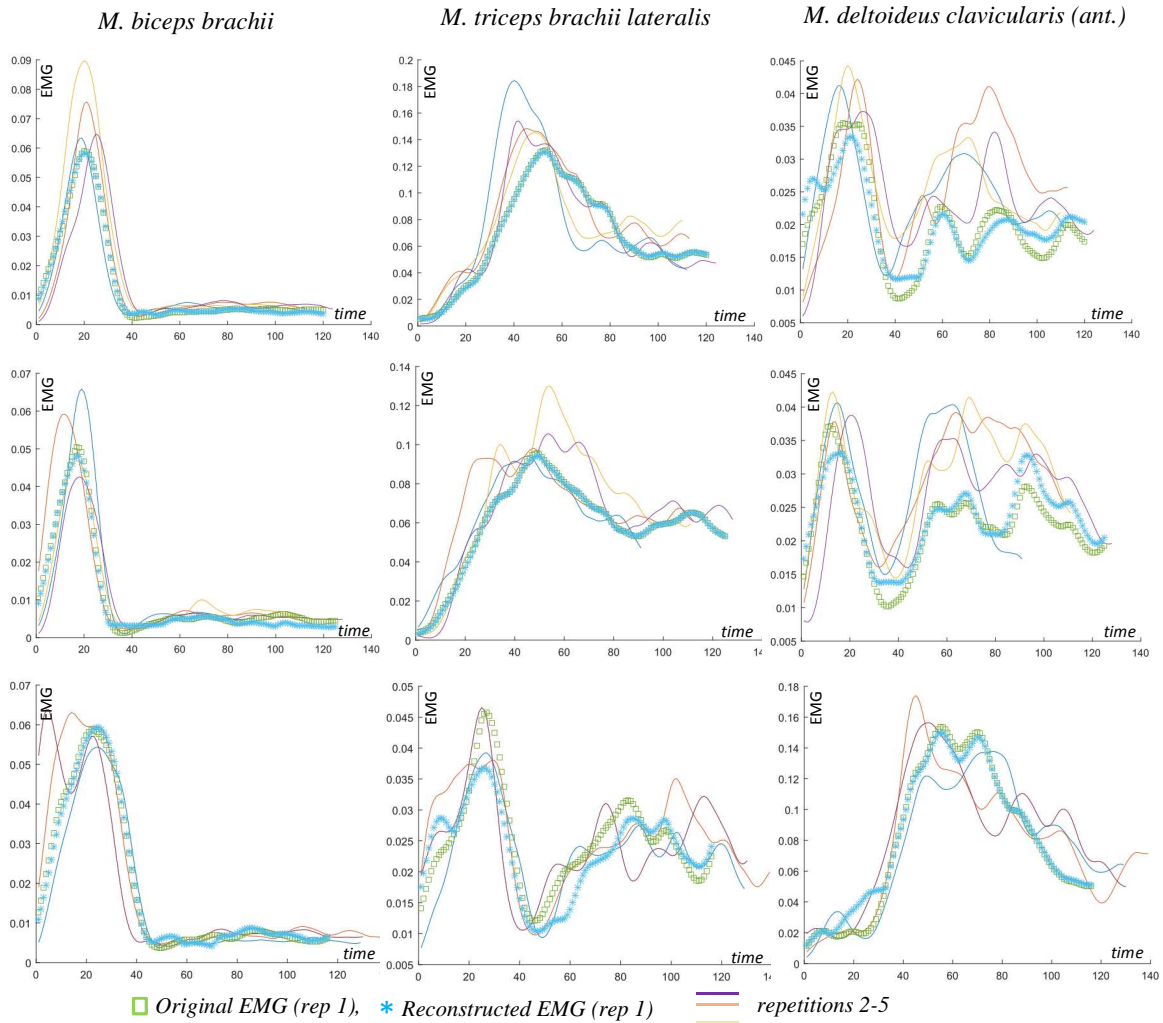


Figure 7: Measured and reproduced EMG signals of the *musculus biceps brachii* (first column), *musculus triceps brachii lateralis* (second column) and *musculus deltoideus clavicularis (anterior)* (third column) for different scenarios (rows).

The original (measured) EMG signals of the first repetition of each task are plotted with green squares. The repetitions 2 - 5 are plotted as purple, orange, yellow and blue lines. The via muscle synergies reproduced EMG signals of the first repetitions are plotted with blue stars. In the first row the signals of the reaching motion to point P1 in test scenario 1 are depicted. For synergy extraction, the Matrix M_a was used, so the signals to be reproduced are involved in the NMF algorithm. In the second row, the signals of the reaching motion to point P2 in test scenario 1 are plotted. For synergy extraction the Matrix M_c is used, hence the reproduced signals are not involved in the NMF algorithm. In the third row the signals of the reaching motion to point P1 in test scenario 10, where motions with weight cuff adjusted to the wrist are measured, are shown. For synergy extraction the Matrix M_{nw} is used, meaning the reproduced signals are not included in the NMF algorithm here as well.

5. Conclusion and future work

An optimal control framework for dynamic and human like motion generation is developed, which allows to exploit the advantages of different DHM actuation modes like joint torque, single muscle and muscle synergy actuation. Further on, measurements in the motion lab were made that allow the validation of the simulation results (trajectories, speed profiles, muscle activation signals). From the measured EMG signals muscle synergies were extracted and validated, that can be used to actuate the DHM. This actuation mode reduces anatomical redundancy, and we expect it to lead to a computational speed up in the musculoskeletal simulation environment. Further on, the spatial characteristics of human muscle activations, captured through muscle synergies, are brought into the simulation process, which can lead to more natural muscle activation patterns. First simulation results are quite promising, and the characteristics of the resulting motions and activation signals for distinct cost functions and the outcomes for mixed cost functions (e.g. to simulate fast vs. precise motion behavior) will be further investigated. Additionally it is planned to measure and simulate further tasks, which include e.g. the interaction with the environment (external forces).

Acknowledgments

This work was supported by the Fraunhofer Internal Programs under Grant No. MAVO 828 424.

References

- [1] N. Bernstein. *The Coordination and Regulation of Movements*. Pergamon Press, Oxford 1967.
- [2] E Bizzi, V.C.K. Cheung, A. d'Avella, P. Saltiel and M. Tresch. Combining modules for movement. *Brain Research Reviews*, Volume 57, Issue 1, Pages 1-270, January 2008.
- [3] E. Todorov. Optimality principles in sensorimotor control. *Nature Neuroscience*, 7: 907 – 915, 2004.
- [4] S. Björkenstam, J. S. Carlson, B. Lennartson. Exploiting sparsity in the discrete mechanics and optimal control method with application to human motion planning. *Eleventh IEEE International Conference on Automation Science and Engineering*, pp.769-774, Gothenburg, Sweden, 2015.
- [5] R. Maas, S. Leyendecker. Biomechanical optimal control of human arm motion. *Journal of Multi-Body Dynamics* 227(4) 375-389, 2013.
- [6] S. Leyendecker, S. Ober-Blöbaum, J. Marsden and M. Ortiz. Discrete mechanics and optimal control for constrained systems. *Optimal control applications & methods*, 31(6), 505–528, 2010.
- [7] M. C. Tresch, V. C. K. Cheung, A. d'Avella. Matrix Factorization Algorithms for the Identification of Muscle Synergies: Evaluation on Simulated and Experimental Data Sets. *Journal of Neurophysiology*, Vol. 95 no. 4, 2199-2212, 2006.
- [8] J. Cholewicki, S. M. McGill, R. W. Norman. Comparison of muscle forces and joint load from an optimization and EMG assisted lumbar spine model: Towards development of a hybrid approach. *Journal of Biomechanics*, Volume 28, Issue 3, Pages 321–325, 327–331, 1995.
- [9] R. Featherstone. *Rigid body dynamics algorithm*. Springer, 2014.
- [10] S. Björkenstam, N. Delfs, J. S. Carlson, R. Bohlin and B. Lennartson. Enhancing digital human motion planning of assembly tasks through dynamics and optimal control. *Procedia CIRP*, 44, 20-25. , 2016.
- [11] S. Björkenstam, S. Leyendecker, J. S. Carlson, and B. Lennartson. Inverse dynamics for discrete mechanics of multibody systems with application to direct optimal control. *Submitted for publication*.
- [12] A. Wächter and L. T. Biegler. On the Implementation of a Primal-Dual Interior Point Filter Line Search Algorithm for Large-Scale Nonlinear Programming, *Mathematical Programming* 106(1), pp. 25-57, 2006.
- [13] P. Konrad. *EMG-FIBEL Eine praxisorientierte Einführung in die kinesiologische Elektromyographie*. Version 1.1, Januar 2011
- [14] Wu, Ge; van der Helm, Frans C.T; Veeger, H.E.J; Makhsous, Mohsen; van Roy, Peter; Anglin, Carolyn et al.: ISB recommendation on definitions of joint coordinate systems of various joints for the reporting of human joint motion—Part II: shoulder, elbow, wrist and hand. *Journal of Biomechanics* 38 (5), S. 981–992. DOI: 10.1016/j.jbiomech.2004.05.042, 2005
- [15] Sint Jan, S. V. *Color atlas of skeletal landmark definitions. Guidelines for reproducible manual and virtual palpations*. Churchill Livingstone/Elsevier, Edinburgh, New York, 2007
- [16] The European Recommendations for Surface Electromyography (SENIAM) Web Link: <http://www.seniam.org/>
- [17] B. Freriks, H.J. Hermens. *European Recommendations for Surface ElectroMyoGraphy, results of the SENIAM project*, ISBN: 90-75452-14-4,1999.
- [18] E. Chiovetto, B. Berret, I. Delis, S. Panzeri, T. Pozzo. Investigating reduction of dimensionality during single-joint elbow movements: a case study on muscle synergies. *Frontiers in Computational Neuroscience*, Vol 7-11, 2016.